element is large and itself sits on the 3 axis. This Coulombic effect would be largest for ternary element M^{3+} and smallest for M^{+}. Therefore, we find La^{3+} producing more chalcogen ordering than does Ag^{+}.

A further point to consider is that, as pointed out by Yvon,[7] the ternary element M may be "delocalized" off the 3 axis, i.e., show large mean-square displacement in directions perpendicular to the 3 axis. This delocalization is favored for small ions such as Cu^{+}, but apparently it is also appreciable for highly polarizable ions such as Ag^{+}. In any case, it is believed that delocalization acts to decrease the chalcogen ordering, as it diminishes the M^{n+} special-position interaction while enhancing the M^{n+} general-position interaction.

A final point to note from Figure 4 is that, aside from the data for Ag^{+} and La^{3+}, the rest of the data roughly cluster together as would be appropriate if all the other ternary elements involved were divalent. This is certainly true for lead[2] and ytterbium.[5] For europium, Mössbauer data[8] reveal a well-defined Eu^{2+} resonance down to 0.5 K. For samarium, the question is still open. It is generally assumed that samarium in these Chevrel phases is trivalent, but these crystallographic data suggest that it is divalent. Magnetic susceptibility studies now in progress should give an unequivocal answer to the question.

Acknowledgment. This research was sponsored by the Air Force Office of Scientific Research through Grant No. 80-0009 and was supported in part by the National Science Foundation and the Materials Science Center at Cornell University.

(7) Yvon, K. *Solid State Commun.* **1978**, *25*, 327.

(8) Fradin, F. Y.; Shenoy, G. K.; Dunlap, B. D.; Aldred, A. T.; Kimball, K. C. *Phys. Rev. Lett.* **1977**, *38*, 719.

Contribution from the Department of Chemistry, University of California, Berkeley, California 94720

Synthesis, Characterization, and Ground Electronic State of the Unstable Monomeric Manganese(IV) Porphyrin Complexes Diazido- and Bis(isocyanato)(5,10,15,20-tetraphenylporphinato)manganese(IV). Crystal and Molecular Structure of the Bis(isocyanato) Complex

MARK J. CAMENZIND, FREDERICK J. HOLLANDER, and CRAIG L. HILL*

Received March 16, 1983

The complexes diazido(5,10,15,20-tetraphenylporphinato)manganese(IV), $Mn^{IV}TPP(N_3)_2$ (**1**), and bis(isocyanato)-(5,10,15,20-tetraphenylporphinato)manganese(IV), $Mn^{IV}TPP(NCO)_2$ (**2**), have been synthesized by reacting $Mn^{IV}TPP(OCH_3)_2$ with either trimethylsilyl azide or isocyanic acid (HNCO) at ~−50 °C. Both **1** and **2** are thermally unstable in solution at room temperature and decompose cleanly to $Mn^{III}TPP(X)$ (X = N_3 or NCO). Variable-temperature magnetic susceptibility measurements, EPR spectroscopy, UV/visible spectroscopy, and infrared spectra of **1** and **2** are distinct from those exhibited by formally isoelectronic Mn(III) tetraphenylporphyrin π cation radical complexes. The properties of **1** and **2** are consistent with a high-spin d^3 Mn(IV) ground electronic state. The infrared spectra of **1** and **2** show unusually low asymmetric stretching frequencies for the azide (ν = 1997 cm^{-1}) and isocyanate (ν = 2127 cm^{-1}) axial ligands. The complexes $Mn^{IV}TPP(X)_2$ (X = OCH_3, N_3, NCO) show highly anisotropic EPR spectra at 12 K that are consistent with a d^3 ion possessing a large zero-field splitting parameter, $|D| > 0.6$ cm^{-1}. Crystals of $Mn^{IV}TPP(NCO)_2 \cdot 0.5C_6H_5CH_3$ were subjected to X-ray crystallographic analysis. The complex crystallized in space group $C2/c$, with cell dimensions a = 21.200 (2) Å, b = 17.582 (2) Å, c = 21.999 (3) Å, β = 108.81 (1)°, V_{calcd} = 7762 (3) Å^3, and Z = 8. The structure was refined by least-squares techniques to a final value of R = 0.0408 (R_w = 0.0512) based on 3027 observations. The coordination about the manganese atom is pseudooctahedral with the average $Mn-N_{pyrrole}$ distance of 1.970 Å and the average $Mn-N_{NCO}$ distance of 1.926 Å. Although the $Mn-N_4$ unit is almost planar, the porphyrin core is distorted into a saddle shape by a large degree of quasi-S_4 ruffling. The average displacement of the meso carbon atoms from the N_4 plane is ±0.59 Å. The torsion angle of the two NCO ligands about the $N_{NCO(A)}-N_{NCO(B)}$ vector is 81.5°. The orientation of the NCO ligands and the ruffling of the porphyrin core can be attributed to crystal-packing forces.

Introduction

High-valent[1] manganese porphyrin complexes have been shown to be capable of oxidizing unactivated hydrocarbon C–H bonds to a variety of products in both stoichiometric and catalytic reactions,[2] and several manganese(IV) porphyrin complexes have recently been isolated from these systems.[3] Other high-valent manganese porphyrin complexes have been shown to be capable of evolving oxygen or hydrogen peroxide in thermal or photochemical reactions.[4] The isolation and determination of the structural and spectroscopic properties of a variety of high-valent manganese porphyrin complexes should greatly facilitate the study of their roles in these interesting reactions. Detailed spectroscopic studies of the complex $Mn^{IV}TPP(O_2)$[5,6] have been reported, and the isolation and X-ray crystallographic characterization of a monomeric Mn(IV)[7] and a monomeric Mn(V)[8] porphyrin complex have

* To whom correspondence should be addressed at the Department of Chemistry, Emory University, Atlanta, GA 30322.

(1) "High-valent" will be used in this paper to refer to manganese porphyrin complexes more oxidized than the manganese(III) porphyrin oxidation state, the stable oxidation state of manganese porphyrin complexes under aerobic conditions.

(2) (a) Smegal, J. A.; Hill, C. L. *J. Am. Chem. Soc.* **1983**, *105*, 3515. (b) Hill, C. L.; Smegal, J. A. *Nouv. J. Chim.* **1982**, *6*, 287. (c) Mansuy, D.; Bartoli, J.-F.; Momenteau, M. *Tetrahedron Lett.* **1982**, *23*, 2781. (d) Chang, C. K.; Ebina, F. *J. Chem. Soc., Chem. Commun.* **1981**, 778. (e) Mansuy, D.; Bartoli, J.-F.; Chottard, J.-C.; Lange, M. *Angew. Chem., Int. Ed. Engl.* **1980**, *19*, 909. (f) Hill, C. L.; Schardt, B. C. *J. Am. Chem. Soc.* **1980**, *102*, 6374. (g) Groves, J. T.; Kruper, W. J., Jr.; Haushalter, R. C. *Ibid.* **1980**, *102*, 6375. (h) Tabushi, I.; Koga, N. *Tetrahedron Lett.* **1979**, *38*, 3681.

(3) (a) Smegal, J. A.; Hill, C. L. *J. Am. Chem. Soc.* **1983**, *105*, 2920. (b) Schardt, B. C.; Hollander, F. J.; Hill, C. L. *Ibid.* **1982**, *104*, 3964. (c) Smegal, J. A.; Schardt, B. C.; Hill, C. L. *Ibid.* **1983**, *105*, 3510.

(4) (a) Harriman, A.; Porter, G. *J. Chem. Soc., Faraday Trans. 2* **1979**, *75*, 1543. (b) Porter, G. *Proc. R. Soc. London, Ser. A* **1978**, *362*, 281. (c) Tabushi, I.; Kojo, S. *Tetrahedron Lett.* **1975**, 305.

0020-1669/83/1322-3776$01.50/0

appeared. We have also recently reported the isolation and characterization of the dimeric manganese porphyrin complexes $[(OCN)Mn^{IV}TPP]_2O$ and $[(N_3)Mn^{IV}TPP]_2O$, including a crystal and molecular structure determination for the latter complex.[3b] In this study we report the isolation and characterization of the related monomeric complexes $Mn^{IV}TPP(N_3)_2$ (**1**) and $Mn^{IV}TPP(NCO)_2$ (**2**). Although recent reports[9] indicate that the oxidation of several $Mn^{III}TPP(X)$ complexes occurs at the porphyrin ligand to give the Mn(III) tetraphenylporphyrin π cation radical complexes $[Mn^{III}TPP(X)](ClO_4)$, complexes **1** and **2** are shown to possess a Mn(IV) porphyrin ground electronic state.

Experimental Section

Physical Measurements. Elemental analyses were performed by the microanalytical laboratory, Department of Chemistry, University of California, Berkeley, CA. Infrared spectra of solid samples 2 wt % in KBr pellets were recorded on a Perkin-Elmer 597 spectrophotometer. The samples were pulverized with the KBr in a "Wig-L-Bug" by shaking for about six 1-s intervals. The use of longer periods of shaking (e.g. 20 s) caused extensive decomposition of the brown Mn(IV) porphyrin complexes to green Mn(III) porphyrin species. The use of a Hewlett-Packard 8450A UV/visible digital spectrometer was essential for recording the spectra of the unstable $Mn^{IV}TPP(X)_2$ complexes since it allows the rapid (2 s) determination of the complete (200–800 nm) electronic spectrum. Variable-temperature magnetic susceptibility measurements in the solid state were recorded on a SQUID apparatus (SHE Corp. VTS 800 susceptometer) that had been calibrated at room temperature by using a Pt standard. The calibration at low temperatures was verified by reproducing the literature susceptibility values[10] of $HgCo(SCN)_4$ to within 1% over the temperature range 5–50 K. X-Band EPR spectra were recorded on a Varian E-109 spectrometer. The field was calibrated with 2,2-diphenyl-1-picrylhydrazyl (DPPH). A temperature of 12 K was obtained with an Air Products Helitran low-temperature accessory.

Materials. $Mn^{IV}TPP(OCH_3)_2$,[7] $Mn^{III}TPP(N_3)$, and $Mn^{III}TPP(NCO)$[3b] were synthesized by literature methods. Methanol was distilled from $Mg(OCH_3)_2$. Dichloromethane, chlorobenzene, toluene, and hexane were purified by washing sequentially with H_2SO_4 (at least three washes), water, and dilute aqueous Na_2CO_3, followed by drying with Na_2SO_4 and fractionally distilling from P_2O_5 under N_2. Chloroform was purified in the same manner and then passed through a short column of activity grade I alumina immediately prior to use. Dichloromethane was stored over activated 4-Å molecular sieves. All solvents were stored in a 5 °C cold room. Isocyanic acid was made by literature methods[11] and was stored at −78 °C. Trimethylsilyl azide was purchased from Petrarch Systems, Inc. Other reagents were used as received.

Methods. Dry and oxygen-free N_2 atmospheres were used routinely, except for the manipulation of solid Mn porphyrin complexes. Manipulations under N_2 were performed by using standard Schlenk, cannula, and syringe techniques. The stabilities of the Mn(IV) porphyrin complexes in solution were found to be extremely sensitive to contact with serum stoppers. For example, when a serum-stoppered test tube containing a brown solution of 0.5 mM $Mn^{IV}TPP(NCO)_2$ in chlorobenzene at 5 °C was shaken for 1 min, complete reduction to green $Mn^{III}TPP(NCO)$ (λ = 476 nm) occurred after an additional 1 min. Another identical solution that was not shaken remained oxidized (brown) 3 days later. Hence, special care was taken to avoid contact of the porphyrin solutions with the serum stoppers, and all serum stoppers were scrubbed with acetone and hexane and then dried in vacuo for at least 12 h. Samples for EPR spectra were made in a −15 °C cold room to minimize thermal decomposition. The porphyrin complexes were accurately weighed into the EPR tubes (4 mm quartz), placed under an N_2 atmosphere, and then serum stoppered. The precooled solvents (−15 °C) were added via syringe, and then the EPR tubes were vigorously shaken for ~1 min and frozen in liquid nitrogen.

Synthesis of $Mn^{IV}TPP(N_3)_2$. The reaction was carried out in a cold room (5 °C) to minimize the potential for thermal decomposition. A typical preparation is as follows: An oven-dried test tube was loaded with 60 mg (0.082 mmol) of $Mn^{IV}TPP(OCH_3)_2$, serum stoppered, purged with N_2, and cooled to −55 °C in a dry ice/isopropyl alcohol bath. The starting material was treated with 4 mL of CH_2Cl_2 via syringe, the reaction mixture was stirred for 1 min, and then 100 μL of $(CH_3)_3SiN_3$ (0.76 mmol) was added via syringe. The solution turned brown instantly. The solution was stirred for 9 min at −55 °C and then filtered through a medium frit into 30 mL of vigorously stirred methanol, also at −55 °C. The mixture was stirred for 11 min, and then the product was collected by filtration. (The visible spectrum of the mother liquors showed only the $[Mn^{III}TPP]^+$ chromophore, λ_{max} = 468 nm.) The precipitate was rinsed with 5 mL of methanol and then dried in vacuo at 25 °C for 9 h to yield 52 mg (82%) of a caked mass of red-purple microcrystals. The product obtained was always solvated with a variable and nonstoichiometric amount of CH_2Cl_2. The amount of solvate was fit on the basis of the Cl analysis. Anal. Calcd for $C_{44}H_{28}N_{10}Mn\cdot0.29CH_2Cl_2$: C, 68.65; H, 3.71; N, 18.08; Cl, 2.45. Found: C, 68.87; H, 3.76; N, 17.63; Cl, 2.45.

Synthesis of $Mn^{IV}TPP(NCO)_2$. $Mn^{IV}TPP(OCH_3)_2$, 300 mg (0.41 mmol), was loaded into a large test tube. The test tube was serum stoppered and purged with N_2. The following operations were performed in a cold room (5 °C) to minimize the potential of thermal decomposition. The starting material was dissolved in 30 mL of CH_2Cl_2, and the solution was cooled to −50 °C. The solution was treated with 150 μL of liquid HNCO (4 mmol) via syringe to yield a deep orange solution (the syringe must be immediately cleaned since HNCO polymerizes rapidly at 5 °C).[11] The solution was stirred for 5 min at −50 °C and then filtered. The filtrate was stirred for 4 min at −50 °C, and then 100 mL of hexane was added dropwise over a 15-min period. The resulting precipitate was collected by filtration, rinsed with hexane, and then dried in vacuo for 40 h at 25 °C to yield 209 mg (64%) of finely divided purple crystals. The amount of CH_2Cl_2 solvate was determined by the chloride analysis. Anal. Calcd for $C_{46}H_{28}N_6MnO_2\cdot0.438CH_2Cl_2$: C, 70.86; H, 3.69; N, 10.69; Mn, 6.99; Cl, 3.71. Found: C, 71.46; H, 3.63; N, 10.82; Mn, 7.11; Cl, 3.71.

X-ray Crystallography. Crystal Growth. The test tubes used for crystal growth were heated to red heat to reduce the number of nucleation sites. They were then serum stoppered and cooled under N_2. A 3.5-mg portion of $Mn^{IV}TPP(NCO)_2$ was dissolved in 7 mL of toluene at 5 °C and filtered into three 1.5 cm × 15 cm test tubes. These solutions were each layered with at least 5 mL of hexane and were left undisturbed at −15 °C for 60 h. The largest shiny black crystal from one of these tubes was mounted on a glass fiber, in air, with polycyanoacrylate glue. The density of the crystals was determined by flotation in CCl_4/hexane mixtures.

Data Collection. Preliminary precession photographs showed monoclinic symmetry and yielded preliminary cell dimensions. Systematic absences (hkl, $h + k \neq 2n$; $h0l$, $l \neq 2n$) were consistent with space groups $C2/c$ or Cc. The former was confirmed by solution and refinement of the structure. The crystal was then mounted on an Enraf-Nonius CAD-4 automated diffractometer and centered in the beam.[12] Automatic peak-search and indexing procedures yielded the same unit cell and absences as the photographs. The final cell dimensions and details of the data collection are given in Table I.

Data Reduction and Refinement. The 5407 raw intensity data were converted to structure factor amplitudes and their esd's by correction for scan speed, background, and Lorentz and polarization effects.[13-15]

(5) Abbreviations used: TPP^{2-}, the dianion of 5,10,15,20-tetraphenylporphyrin; OEP^{2-}, the dianion of octaethylporphyrin; HIm, imidazole; MesoPDME, the dimethyl ester of mesoporphyrin IX; en, ethylenediamine.

(6) Hoffman, B. M.; Szymanski, T.; Brown, T. G.; Basolo, F. *J. Am. Chem. Soc.* **1978**, *100*, 7253 and references cited therein.

(7) Camenzind, M. J.; Hollander, F. J.; Hill, C. L. *Inorg. Chem.* **1982**, *21*, 4301.

(8) Hill, C. L.; Hollander, F. J. *J. Am. Chem. Soc.* **1982**, *104*, 7318.

(9) (a) Goff, H. M.; Phillippi, M. A.; Boersma, A. D.; Hansen, A. P. *Adv. Chem. Ser.* **1982**, *No. 201*, 357. (b) Kelley, S. L.; Kadish, K. M. *Inorg. Chem.* **1982**, *21*, 3631.

(10) Brown, D. B.; Crawford, V. H.; Hall, J. W.; Hatfield, W. E. *J. Phys. Chem.* **1977**, *81*, 1303.

(11) Glemser, O. In "Handbook of Preparative Inorganic Chemistry", 2nd ed.; Brauer, G., Ed.; Academic Press: New York, 1963; Vol. 1, p 667.

(12) Instrumentation at the University of California Chemistry Department X-ray Crystallographic Facility (CHEXRAY) consists of two Enraf-Nonius CAD-4 diffractometers, one controlled by a DEC PDP 8/a with a RK05 disk and the other by a DEC PDP 8/e with an RL01 disk. Both use Enraf-Nonius software as described in: "CAD-4 Operation Manual"; Enraf-Nonius: Delft, The Netherlands, 1977 (updated Jan 1980).

(13) All calculations were performed on a PDP 11/60 using locally modified Nonius-SDP[14] software.

Table I. Crystal and Data Collection Parameters for $Mn^{IV}TPP(NCO)_2 \cdot {}^1/_2C_6H_5CH_3$

(A) Crystal Parameters at 25 °C[a,b]	
formula	$C_{49.5}H_{32}N_6O_2Mn$
fw	797.78
space group	$C2/c$
a, Å	21.200 (2)
b, Å	17.582 (2)
c, Å	21.999 (3)
β, deg	108.81 (1)
V, Å^3	7762 (3)
Z	8
d(calcd), g cm^{-3}	1.37
d(obsd), g cm^{-3}	1.34
cryst dimens, mm	0.13 × 0.14 × 0.23
μ(calcd), cm^{-1}	3.74
(B) Data Collection	
diffractometer	Enraf-Nonius CAD-4
radiation	Mo Kα ($\bar{\lambda}$ = 0.710 73 Å)
monochromator	highly-oriented graphite ($2\theta_m$ = 12.2°) perpendicular mode, assumed 50% perfect
detector	cryst scintillation counter, with PHA
horizontal aperture, mm	2 + tan θ (variable)
reflcns measd	$+h, +k, \pm l$
scan type	θ–2θ
2θ range, deg	3–45
scan speed, deg min^{-1}	0.6–6.7
scan width, deg	$\Delta\theta$ = 0.50 + 0.347 tan θ
bkgd	added 25% of scan width at end of each scan
reflcns collected	5407
unique reflcns	5054
intens stds	(0,8,0), ($\bar{2}$,0,12), (10,0,$\bar{2}$); measd every 2 h of X-ray exposure time; over the period of data collection no decay in intens obsd
orientation	3 reflcns checked after every 250 measmts; cryst orientation was redetermined if any reflcns were offset from their predicted positions by more than 0.1°; reorientation performed once during data collection

[a] Unit cell parameters and their esd's were derived by a least-squares fit to the setting angles of the unresolved Mo K$\bar{\alpha}$ components of 24 reflections with 2θ near 28°. [b] In this and all subsequent tables the esd's of all parameters are given in parentheses for the least significant digit(s) given.

No crystal decomposition was observed. Inspection of the azimuthal scan data[16] showed only a ±2.5% variation in intensity, so no absorption correction was performed. Following removal of systematically absent and redundant reflections, 5054 unique data remained. Of these, the 3027 that had $F_o^2 > 3\sigma(F_o^2)$ were used in least-squares refinement.

The structure was solved by interpretation of the Patterson map and was refined via standard least-squares and Fourier techniques. After refinement of all atoms in the molecule using isotropic thermal parameters, a large region of electron density near $^1/_2$, $^1/_2$, $^1/_2$ was interpreted as a disordered toluene of solvation. This was modeled with seven half-occupancy carbon atoms whose positional parameters were allowed to refine but whose isotropic thermal parameters were fixed. A subsequent difference Fourier map showed peaks near the expected locations for hydrogen atoms. These were included in their idealized positions (C–H = 0.95 Å) in the structure factor calculations but were not refined. Just before the final cycles of least-squares refinement the isotropic thermal parameter for the toluene solvate

Table II. Final Positional Parameters[a] for the Non-Hydrogen Atoms of $MnTPP(NCO)_2 \cdot {}^1/_2C_6H_5CH_3$

atom	x	y	z	B, Å^2
Mn	0.31064 (3)	0.10736 (4)	0.30861 (3)	3.08 (1)
N1	0.3623 (2)	0.1530 (2)	0.2580 (2)	3.06 (9)
N2	0.3347 (2)	0.0049 (2)	0.2871 (2)	3.14 (8)
N3	0.2594 (2)	0.0608 (2)	0.3596 (2)	3.28 (9)
N4	0.2070 (2)	0.2096 (2)	0.3308 (2)	3.02 (8)
C1	0.3835 (2)	0.2277 (3)	0.2611 (2)	3.1 (1)
C2	0.4161 (2)	0.2385 (3)	0.2141 (2)	3.7 (1)
C3	0.4130 (2)	0.1726 (3)	0.1820 (2)	3.7 (1)
C4	0.3815 (2)	0.1180 (3)	0.2107 (2)	3.2 (1)
C5	0.3775 (2)	0.0401 (3)	0.1991 (2)	3.3 (1)
C6	0.3606 (2)	−0.0124 (3)	0.2390 (2)	3.3 (1)
C7	0.3758 (2)	−0.0918 (3)	0.2425 (2)	4.0 (1)
C8	0.3609 (2)	−0.1210 (3)	0.2926 (2)	3.9 (1)
C9	0.3334 (2)	−0.0613 (3)	0.3197 (2)	3.3 (1)
C10	0.3024 (2)	−0.0694 (3)	0.3668 (2)	3.3 (1)
C11	0.2635 (2)	−0.0129 (3)	0.3813 (2)	3.4 (1)
C12	0.2164 (2)	−0.0235 (3)	0.4141 (2)	4.3 (1)
C13	0.1820 (2)	0.0416 (3)	0.4104 (2)	4.4 (1)
C14	0.2103 (2)	0.0958 (3)	0.3784 (2)	3.5 (1)
C15	0.1975 (2)	0.1738 (3)	0.3740 (2)	3.6 (1)
C16	0.2370 (2)	0.2265 (3)	0.3561 (2)	3.4 (1)
C17	0.2397 (2)	0.3069 (3)	0.3694 (2)	4.0 (1)
C18	0.2913 (2)	0.3368 (3)	0.3544 (2)	4.0 (1)
C19	0.3203 (2)	0.2763 (3)	0.3283 (2)	3.3 (1)
C20	0.3688 (2)	0.2849 (3)	0.2985 (2)	3.1 (1)
C21	0.3989 (2)	0.0101 (3)	0.1453 (2)	3.3 (1)
C22	0.4650 (2)	0.0074 (3)	0.1487 (2)	4.8 (1)
C23	0.4834 (2)	−0.0212 (3)	0.0992 (2)	5.6 (1)
C24	0.4371 (2)	−0.0462 (3)	0.0449 (2)	5.2 (1)
C25	0.3713 (3)	−0.0450 (3)	0.0401 (2)	5.9 (2)
C26	0.3515 (2)	−0.0163 (3)	0.0900 (2)	4.9 (1)
C27	0.3066 (2)	−0.1449 (3)	0.3995 (2)	3.6 (1)
C28	0.3546 (3)	−0.1577 (3)	0.4570 (3)	6.0 (2)
C29	0.3583 (3)	−0.2267 (4)	0.4879 (3)	7.5 (2)
C30	0.3130 (3)	−0.2824 (3)	0.4621 (3)	5.8 (2)
C31	0.2659 (3)	−0.2708 (3)	0.4055 (3)	6.8 (2)
C32	0.2626 (3)	−0.2020 (3)	0.3738 (3)	6.1 (2)
C33	0.1411 (2)	0.2033 (3)	0.3944 (2)	4.0 (1)
C34	0.0807 (3)	0.2165 (4)	0.3489 (3)	6.4 (2)
C35	0.0280 (3)	0.2427 (4)	0.3676 (4)	8.8 (2)
C36	0.0364 (3)	0.2577 (4)	0.4302 (3)	8.0 (2)
C37	0.0959 (3)	0.2459 (4)	0.4744 (3)	8.0 (2)
C38	0.1482 (2)	0.2182 (4)	0.4572 (2)	6.1 (2)
C39	0.4038 (2)	0.3593 (3)	0.3030 (2)	3.5 (1)
C40	0.3735 (2)	0.4225 (3)	0.2693 (3)	5.1 (1)
C41	0.4098 (3)	0.4900 (3)	0.2758 (3)	6.4 (2)
C42	0.4735 (3)	0.4944 (3)	0.3156 (3)	6.6 (2)
C43	0.5044 (3)	0.4312 (4)	0.3488 (3)	6.7 (2)
C44	0.4695 (2)	0.3634 (3)	0.3425 (3)	5.3 (1)
N(A)	0.3891 (2)	0.1096 (2)	0.3840 (2)	3.70 (9)
C(A)	0.4393 (2)	0.1435 (3)	0.4009 (2)	4.0 (1)
O(A)	0.4912 (2)	0.1761 (2)	0.4212 (2)	6.7 (1)
N(B)	0.2336 (2)	0.1059 (2)	0.2330 (2)	4.2 (1)
C(B)	0.1861 (3)	0.1436 (3)	0.2155 (3)	5.4 (1)
O(B)	0.1343 (2)	0.1800 (3)	0.1947 (2)	9.2 (1)
C45	0.4704 (6)	0.4392 (7)	0.5042 (6)	7.0*
C46	0.5503 (6)	0.4232 (7)	0.5429 (6)	7.0*
C47	0.5888 (6)	0.4781 (7)	0.5456 (6)	7.0*
C48	0.5720 (6)	0.5453 (7)	0.5212 (6)	7.0*
C49	0.4975 (6)	0.5662 (7)	0.4818 (6)	7.0*
C50	0.4596 (5)	0.5067 (7)	0.4822 (6)	7.0*
C51	0.3689 (6)	0.5256 (7)	0.4368 (6)	7.0*

[a] Values marked with an asterisk are isotropic thermal parameters. Anisotropically refined atoms are given in the form of the isotropic equivalent thermal parameter defined as $^4/_3[a^2B_{11} + b^2B_{22} + c^2B_{33} + ab(\cos\gamma)B_{12} + ab(\cos\beta)B_{13} + bc(\cos\alpha)B_{23}]$.

(14) "Structure Determination Package User's Guide"; Molecular Structure Corporation: College Station, TX, 1980.

(15) The data reduction formulas are

$$F_o^2 = \frac{\omega}{Lp}(C - 2B) \qquad \sigma_o(F_o^2) = \frac{\omega}{Lp}(C + 4B)^{1/2} \qquad F_o = (F_o^2)^{1/2}$$

$$\sigma_o(F) = \frac{\sigma_o(F_o^2)}{2F_o}$$

where C is the total count in the scan, B is the sum of the two background counts, ω is the scan speed used in deg/min, and

$$\frac{1}{Lp} = \frac{(\sin 2\theta)(1 + \cos^2 2\theta_m)}{1 + \cos^2 2\theta_m - \sin^2 2\theta}$$

is the correction for Lorentz and polarization effects for a reflection with scattering angle 2θ and radiation monochromatized with a 50% perfect single-crystal monochromator with scattering angle $2\theta_m$.

(16) Reflections used for azimuthal scans were located near χ = 90°, and the intensities were measured at 10° increments of rotation of the crystal about the diffraction vector.

was increased from 6.0 to 7.0 Å^2 to produce a "flatter" difference Fourier in that region. No attempt was made to refine the occupancy of the toluene solvate.

The final residuals for 517 variables refined against the 3027 data for which $F_o^2 > 3\sigma(F_o^2)$ were $R = 0.0408$, $R_w = 0.0512$, and GOF = 1.996.[17] The R value for all 5054 data was 0.108. The quantity minimized by the least-squares program was $\sum w(|F_o| - |F_c|)^2$, where w is the weight of a given observation. The p factor,[17] used to reduce the weight of intense reflections, was set to 0.03 throughout the refinement. The analytical forms of the scattering factor tables for the neutral atoms were used,[18] and all non-hydrogen scattering factors were corrected for both the real and the imaginary components of anomalous dispersion.[19]

Inspection of the residuals ordered in ranges of $(\sin\theta)/\lambda$, $|F_o|$, parity, and the value of the individual indexes showed no unusual features or trends. There was no evidence of secondary extinction in the low-angle, high-intensity data.

The largest peak in the final difference Fourier map had an electron density of 0.38 e/Å^3 and was located near the toluene solvate molecule.

The final positional parameters of the non-hydrogen atoms are given in Table II. The thermal parameters of the non-hydrogen atoms, the positions of the hydrogen atoms, and a listing of the values of F_o and F_c are available as supplementary material.

Results

Synthesis and Stability. The syntheses of the complexes $Mn^{IV}TPP(X)_2$ (X = N_3, NCO) require the use of low temperatures to minimize thermal decomposition to $Mn^{III}TPP(X)$. Even at low temperatures, the reaction of HNCO or $(CH_3)_3SiN_3$ with $Mn^{IV}TPP(OCH_3)_2$ is always accompanied by some formation of the corresponding $Mn^{III}TPP(X)$ (X = N_3, NCO) complex (based on the visible spectra). In the synthesis of $Mn^{IV}TPP(NCO)_2$, the less soluble $Mn^{IV}TPP(NCO)_2$ product can be precipitated with hexane while the more soluble $Mn^{III}TPP(NCO)$ is left in solution. In the case of $Mn^{IV}TPP(N_3)_2$, however, attempts to precipitate $Mn^{IV}TPP(N_3)_2$ from chlorocarbon solutions with hexane always resulted in the coprecipitation of $Mn^{III}TPP(N_3)$. Since $Mn^{IV}TPP(N_3)_2$ is insoluble in methanol and $Mn^{III}TPP(N_3)$ dissolves in methanol to give the characteristic $[Mn^{III}TPP]^+$ cation (λ_{max} = 468 nm),[7] the use of excess methanol as the precipitating solvent allowed a clean separation of these two species. $Mn^{IV}TPP(N_3)_2$ could be synthesized by the reaction of $Mn^{IV}TPP(OCH_3)_2$ with either $(CH_3)_3Si(N_3)$ or solutions of HN_3, but the use of HN_3 was less convenient due to its toxicity, volatility, and explosiveness. When the isolated $Mn^{IV}TPP(X)_2$ (X = N_3, NCO) complexes were dissolved in CH_2Cl_2, the visible spectra of the solutions (~0.25 mM) showed isosbestic decompositions to the corresponding $Mn^{III}TPP(X)$ complexes with reduction half-lives of ~40 min for $Mn^{IV}TPP(N_3)_2$ and ~5 h for $Mn^{IV}TPP(NCO)_2$. The fate of the axial ligands has not been determined. The stability of the Mn(IV) complexes in solution is greatly decreased by the presence of trace HCl or H_2O in the solvent. In the solid state, single crystals of the toluene solvate of **2** were stable for weeks, but if these crystals were crushed, reduction to a green Mn(III) porphyrin complex occurred in 24 h.

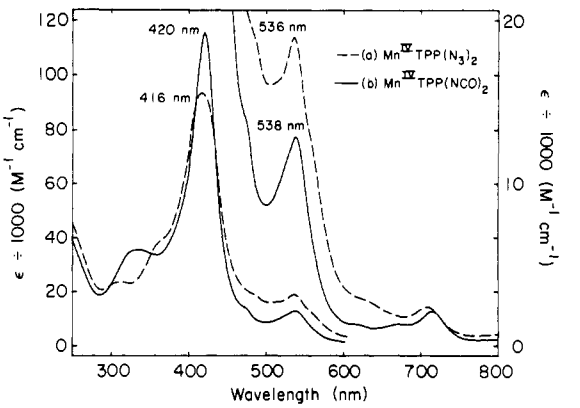

Figure 1. Visible spectra of $Mn^{IV}TPP(NCO)_2$ (0.285 mM) and $Mn^{IV}TPP(N_3)_2$ (0.25 mM) in CH_2Cl_2.

Visible Spectroscopy. The type of visible spectra seen in the $Mn^{IV}TPP(X)_2$ complexes (Figure 1) is clearly distinct from the spectra exhibited by the corresponding $Mn^{III}TPP(X)$ species (in CH_2Cl_2 solution, the $Mn^{III}TPP(X)$ complexes exhibit λ_{max} = 484 nm for X = N_3 and 474 nm for X = NCO). Thus, the visible spectra of the $Mn^{IV}TPP(X)_2$ complexes provide a convenient method for determining the extent of decomposition to the corresponding Mn(III) complexes.

Infrared Spectroscopy. In addition to absorptions normally seen in manganese tetraphenylporphyrin complexes,[3b,7,20] the IR spectra of the **1** and **2** (in KBr pellets, Figure S2)[21] show absorptions characteristic of their respective axial ligands. No characteristic methoxide IR absorptions[7] at 2775, 1050, or 550 cm^{-1} are observed, indicating that the methoxide ligands of the starting material were completely displaced. The diazide complex shows a very intense azide asymmetric stretching band at 1997 cm^{-1}, medium-intensity bands at 1303 and 1255 cm^{-1} that may be azide symmetric stretches,[22] and a Mn–N_3 stretch[22,23] at 418 cm^{-1}. The azide asymmetric stretching band in $Mn^{IV}TPP(N_3)_2$ occurs at a lower energy than in $Mn^{III}TPP(N_3)$ (2033 cm^{-1}),[3b] indicating that a Mn(III) ion is not present. The complex $Mn^{IV}TPP(NCO)_2$ exhibits absorptions at 428 and 446 cm^{-1} that are consistent with Mn–N_{NCO} stretches.[22] The isocyanate asymmetric stretch is found at 2127 cm^{-1} in **2** vs. 2165 cm^{-1} in $Mn^{III}TPP(NCO)$,[3b] again indicating that a Mn(III) ion is not present.

The asymmetric stretches for terminal azide and isocyanate ligands normally occur at significantly higher energies than found in **1** and **2**, suggesting a strong interaction of the pseudohalide ligands with the Mn(IV) ion.[24] The unusually low energies for the pseudohalide absorptions in **1** and **2** may

(17) Residuals and goodness of fit are defined as

$$R = \frac{\sum||F_o| - |F_c||}{\sum|F_o|} \qquad R_w = \left[\frac{\sum w(|F_o| - |F_c|)^2}{\sum wF_o^2}\right]^{1/2}$$

$$\text{GOF} = \left[\frac{\sum w(|F_o| - |F_c|)^2}{n_o - n_v}\right]^{1/2}$$

where n_o is the number of observations, n_v is the number of variable parameters, and the weights w were given by

$$w = \frac{4F_o^2}{\sigma^2(F_o^2)} \qquad \sigma^2(F_o^2) = [\sigma_o^2(F_o^2) + (pF^2)^2]$$

where p is the factor used to lower the weight of intense reflections.

(18) Cromer, D. T.; Waber, J. T. "International Tables for X-ray Crystallography"; Kynoch Press: Birmingham, England, 1974; Vol. IV, Table 2.2B.

(19) Cromer, D. T. "International Tables for X-ray Crystallography"; Kynoch Press: Birmingham, England, 1974; Vol. IV, Table 2.3.1.

(20) Alben, J. O.; Choi, S. S.; Adler, A. D.; Caughey, W. S. *Ann. N.Y. Acad. Sci.* **1973**, *206*, 278.

(21) Available as supplementary material.

(22) (a) Maslowsky, E. "Vibrational Spectra of Organometallic Compounds"; Wiley: New York, 1977. (b) Nakamoto, K. "Infrared and Raman Spectra of Inorganic and Coordination Compounds", 3rd ed.; Wiley: New York, 1978.

(23) An Fe–N_3 stretch at 421 cm^{-1} has been rigorously assigned in the complex $Fe^{III}OEP(N_3)$: Ogoshi, H.; Watanabe, E.; Yoshida, Z.; Kincaid, H.; Nakamoto, K. *J. Am. Chem. Soc.* **1973**, *95*, 2845.

(24) The azide asymmetric stretch for covalently bound terminal azido groups in both organic[25] and organometallic[22] azido complexes normally occurs above 2020 cm^{-1}. The azide asymmetric stretch in ionic azides also normally occurs above 2020 cm^{-1}; e.g., in KN_3, the azide asymmetric stretch is found at 2041 cm^{-1}.[22b] Asymmetric stretches in isocyanate complexes usually occur between 2170 and 2300 cm^{-1}.[22]

(25) Dolphin, D.; Wick, A. "Tabulation of Infrared Spectral Data"; Wiley: New York, 1977.

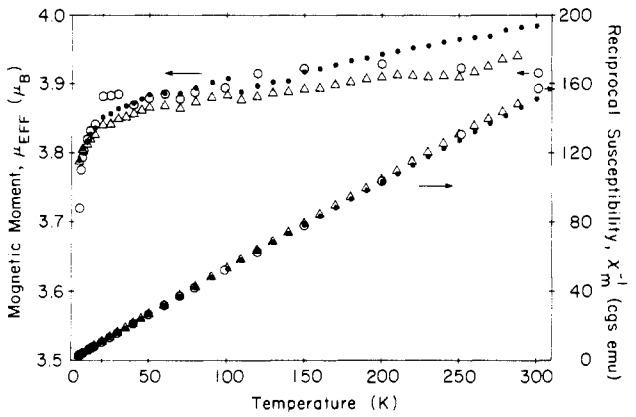

Figure 2. Plots of the effective magnetic moments and inverse corrected molar susceptibility vs. temperature (from 5 to 300 K) for the complexes $Mn^{IV}TPP(X)_2$ (X = OCH_3 (○), N_3 (●), NCO (△)). The data for $Mn^{IV}TPP(OCH_3)_2$ were taken from ref 7.

be due to the mixing of the metal and axial ligand based π orbitals. The low-spin complex $Fe^{III}TPP(N_3)(py)$[26] has been reported to exhibit also an unusually low-energy azide absorption at 2000 cm^{-1}. In this iron porphyrin complex, π bonding between the azide ligand and the metal ion has been suggested.[27]

The energies of the asymmetric stretches in the monomeric Mn(IV) complexes are distinct from those observed in the corresponding μ-oxo dimers, $[XMn^{IV}TPP]_2O$, where these bands are found at 2160 cm^{-1} (X = NCO) and 2010 cm^{-1} (X = N_3).[3b] No strong characteristic tetraphenylporphyrin π cation radical infrared absorptions between 1270 and 1295 cm^{-1} are observed in either **1** or **2**, consistent with the absence of ligand-centered oxidation.[28]

Magnetic Properties. Variable-temperature magnetic susceptibility measurements on **1** and **2** at a field strength of 5000 G were performed on the solid materials from 5 to 300 K.[21] The molar susceptibilities were corrected for the diamagnetism of the TPP ligand,[29] the Mn(IV) ion,[30] the pseudohalide ligands (the susceptibility of CNO[30] was assumed for both NCO and N_3), and the CH_2Cl_2 solvate.[31] No attempt was made to estimate the temperature-independent paramagnetic (TIP) term[32] since the energies of the excited states are not known. Plots of the inverse corrected molar susceptibilities vs. temperature yielded nearly straight lines, indicating approximate Curie–Weiss behavior (Figure 2). The temperature intercepts of these plots based on the low-temperature data (5–25 K) gave very small experimental Weiss constants of −0.2 K for $Mn^{IV}TPP(N_3)_2$ and −0.35 K for $Mn^{IV}TPP(N_3)_2$, which are comparable to that exhibited by $Mn^{IV}TPP(OCH_3)_2$ (θ_w = −0.5 K).[7] The slight increase of the room-temperature magnetic moments above the spin-only magnetic moment expected for a d^3 ion (μ_{so} = 3.87 μ_B) may be due to the presence of trace amounts of high-spin (S = 2) $Mn^{III}TPP(X)$ species, especially for $Mn^{IV}TPP(N_3)_2$. The magnetic moments are in the range $3.8 < \mu_{eff} < 4.0$ μ_B usually found experimentally for Mn(IV) complexes.[33]

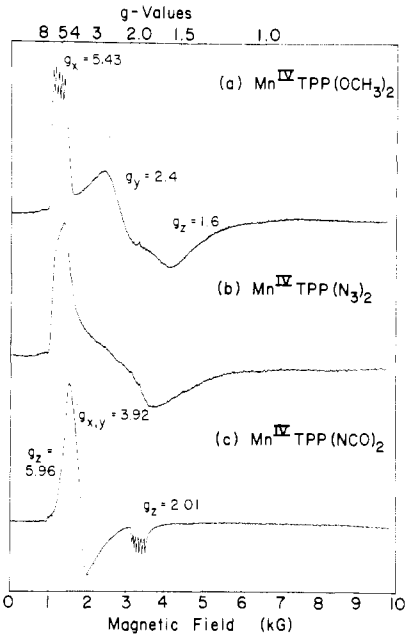

Figure 3. X-Band EPR spectra (9.200 GHz) of $Mn^{IV}TPP(X)_2$ (X = OCH_3, N_3, NCO) in 60/40 v/v toluene/chloroform glasses at 12 K. The spectrometer parameters were as follows: modulation frequency 100 kHz, modulation amplitude 12.5 G, time constant 0.064 s, scan time 8 min, microwave power 5–10 mW, and spectrometer gain 5000 (12 500 for $Mn^{IV}TPP(N_3)_2$). The approximate concentrations were 1 mM for $Mn^{IV}TPP(NCO)_2$ and $Mn^{IV}TPP(OCH_3)_2$ and 2 mM for $Mn^{IV}TPP(N_3)_2$. No attempt has been made to assign any effective g values in the spectrum of $Mn^{IV}TPP(N_3)_2$.

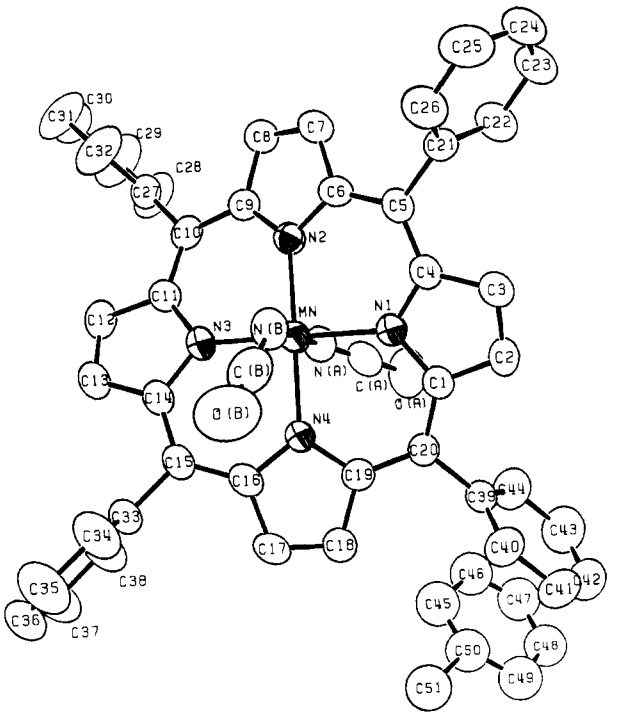

Figure 4. Labeling diagram for $MnTPP(NCO)_2 \cdot {}^1/_2C_6H_5CH_3$. Only one of the two disordered toluene molecules is shown.

EPR Spectroscopy. The complexes $Mn^{IV}TPP(X)_2$ (X = N_3, NCO, and OCH_3) all exhibit highly anisotropic EPR spectra in glassing media at 12 K (Figure 3). The EPR spectra are consistent with a high-spin d^3 ion in a distorted pseudooctahedral environment (see Discussion). Hyperfine coupling to the $I = {}^5/_2$ ^{55}Mn nucleus is resolved in both $Mn^{IV}TPP(OCH_3)_2$

(26) Adams, K. M.; Rasmussen, P. G.; Scheidt, W. R.; Hatano, K. *Inorg. Chem.* **1979**, *18*, 1892.
(27) Scheidt, W. R. In "The Porphyrins"; Dolphin, D., Ed.; Academic Press: New York, 1979; Vol. 3, Chapter 10.
(28) Shimomura, E. T.; Phillippi, M. A.; Goff, H. M.; Scholz, W. F.; Reed, C. A. *J. Am. Chem. Soc.* **1981**, *103*, 6778.
(29) Eaton, S. S.; Eaton, G. R. *Inorg. Chem.* **1980**, *19*, 1095.
(30) König, E.; König, G. In Landolt-Börnstein, "Numerical Data and Functional Relationships in Science and Technology"; Springer-Verlag: New York, 1981; New Series, Group II, Vol. 11, Suppl. 3, p 27.
(31) Smith, G. W. In "Handbook of Chemistry and Physics", 54th ed.; Weast, R. C., Ed.; CRC Press: Cleveland, OH, 1973; p E-128.
(32) Jolly, W. L. "Synthesis and Characterization of Inorganic Compounds"; Prentice-Hall: Englewood Cliffs, NJ, 1970; p 378.
(33) König, E.; König, G. In ref 30, p 10.

Table III. Bond Distances (Å) and Bond Angles (deg) in $MnTPP(NCO)_2 \cdot {}^1/_2C_6H_5CH_3$

atom 1	atom 2	dist	atom 1	atom 2	dist	atom 1	atom 2	dist
Mn	N1	1.968 (3)	C1	C2	1.430 (4)	C10	C9	1.401 (4)
Mn	N2	1.970 (3)	C3	C4	1.428 (4)	C10	C11	1.392 (5)
Mn	N3	1.972 (3)	C6	C7	1.427 (5)	C15	C14	1.395 (5)
Mn	N4	1.969 (3)	C8	C9	1.421 (4)	C15	C16	1.389 (5)
Mn	N(A)	1.934 (3)	C11	C12	1.421 (5)	C20	C1	1.396 (4)
Mn	N(B)	1.918 (3)	C13	C14	1.424 (5)	C20	C19	1.394 (4)
N1	C1	1.381 (4)	C16	C17	1.439 (5)	C5	C21	1.494 (4)
N1	C4	1.377 (4)	C18	C19	1.437 (4)	C10	C27	1.497 (5)
N2	C6	1.374 (4)	C2	C3	1.348 (5)	C15	C33	1.496 (5)
N2	C9	1.373 (4)	C7	C8	1.341 (5)	C20	C39	1.491 (4)
N3	C11	1.373 (4)	C12	C13	1.344 (5)	N(A)	C(A)	1.171 (5)
N3	C14	1.383 (4)	C17	C18	1.348 (5)	C(A)	O(A)	1.193 (5)
N4	C16	1.379 (4)	C5	C4	1.390 (4)	N(B)	C(B)	1.164 (5)
N4	C19	1.378 (4)	C5	C6	1.397 (4)	C(B)	O(B)	1.223 (5)

atom 1	atom 2	atom 3	angle	atom 1	atom 2	atom 3	angle
N(A)	Mn	N1	89.71 (11)	C11	N3	C14	106.5 (3)
N(A)	Mn	N2	90.39 (12)	N3	C11	C12	108.9 (3)
N(A)	Mn	N3	90.01 (12)	N3	C14	C13	109.1 (3)
N(A)	Mn	N4	89.18 (12)	C11	C12	C13	108.2 (3)
N(A)	Mn	N(B)	179.05 (13)	C12	C13	C14	107.1 (3)
N(B)	Mn	N1	89.34 (12)	C16	N4	C19	107.6 (3)
N(B)	Mn	N2	89.61 (13)	N4	C16	C17	108.0 (3)
N(B)	Mn	N3	90.94 (12)	N4	C19	C18	108.9 (3)
N(B)	Mn	N4	90.82 (12)	C16	C17	C18	108.4 (3)
N1	Mn	N3	179.47 (12)	C17	C18	C19	107.1 (3)
N2	Mn	N4	179.55 (12)	C5	C4	N1	124.2 (3)
Mn	N1	C1	126.16 (22)	C5	C4	C3	126.2 (3)
Mn	N1	C4	126.78 (23)	C4	C5	C6	123.3 (3)
Mn	N2	C6	125.94 (23)	C4	C5	C21	118.5 (3)
Mn	N2	C9	126.78 (23)	C6	C5	C21	117.9 (3)
Mn	N3	C11	127.16 (23)	C5	C6	N2	125.6 (3)
Mn	N3	C14	126.27 (23)	C5	C6	C7	125.6 (3)
Mn	N4	C16	125.95 (24)	C10	C9	N2	124.5 (3)
Mn	N4	C19	126.34 (22)	C10	C9	C8	126.1 (3)
Mn	N(A)	C(A)	136.5 (3)	C9	C10	C11	123.4 (3)
Mn	N(B)	C(B)	133.1 (3)	C9	C10	C27	118.4 (3)
N(A)	C(A)	O(A)	176.5 (4)	C11	C10	C27	118.0 (3)
N(B)	C(B)	O(B)	176.3 (5)	C10	C11	N3	124.7 (3)
C1	N1	C4	107.0 (3)	C10	C11	C12	126.0 (3)
N1	C1	C2	108.4 (3)	C15	C14	N3	124.4 (3)
N1	C4	C3	109.2 (3)	C15	C14	C13	126.0 (3)
C1	C2	C3	108.2 (3)	C14	C15	C16	123.6 (3)
C2	C3	C4	107.2 (3)	C14	C15	C33	118.4 (3)
C6	N2	C9	107.1 (3)	C16	C15	C33	117.8 (3)
N2	C6	C7	108.3 (3)	C15	C16	N4	125.7 (3)
N2	C9	C8	109.0 (3)	C15	C16	C17	125.8 (3)
C6	C7	C8	108.1 (3)	C20	C1	N1	125.7 (3)
C7	C8	C9	107.4 (3)	C20	C1	C2	125.5 (3)
				C1	C20	C19	122.5 (3)
				C1	C20	C39	118.1 (3)
				C19	C20	C39	119.3 (3)
				C20	C19	N4	125.1 (3)
				C20	C19	C18	125.7 (3)

($a_{Mn} \approx 72$ G at $g \approx 5.43$) and $Mn^{IV}TPP(NCO)_2$ ($a_{Mn} \approx 69$ G at $g \approx 2$ and $a_{Mn} \approx 68$ G at $g = 5.96$). The weak transition at $g = 5.96$ in $Mn^{IV}TPP(NCO)_2$ probably corresponds to a formally spin-forbidden $\Delta m = 3$ transition. These transitions have been observed in other d^3 complexes.[34]

Description of the Structure. A drawing of $MnTPP(NCO)_2 \cdot {}^1/_2C_6H_5CH_3$ showing the atom-numbering scheme is given in Figure 4, and selected bond distances and angles are given in Table III. A stereoview of the crystal packing in the unit cell is shown in Figure S1.[21]

The inner coordination sphere about the manganese atom is pseudooctahedral, with all N–Mn–N angles within 1° of either 90 or 180°.[21] The NCO groups are ordered, and the internal distances in them are consistent with *N*CO rather than *O*CN binding (see Discussion). The NCO's are nearly linear with the average N–C–O angle of 176.4°. The ordering of the NCO's and their orientation with respect to each other can be attributed to crystal-packing forces. The six NCO atoms participate in 8 of the 12 intermolecular contacts[21] less than 3.51 Å. The isocyanate ligands bind to the Mn in a bent fashion with an average Mn–N–C angle of 134.8°. The torsion angles of the NCO ligands with respect to the nearest $Mn-N_{pyrrole}$ vectors are N1–Mn–N(A)–C(A) = 21.9° and N4–Mn–N(B)–C(B) = −13.4°. The torsion angle C(A)–N(A)–N(B)–C(B) is −81.5°. Since both enantiomers of the molecule are present in the crystal, only the absolute values of these torsion angles are significant.

The four pyrrole nitrogen atoms bound to the manganese ion are coplanar to ±0.001 Å with the Mn atom out of plane by only 0.006 Å toward N(B). The rest of the molecule is

(34) Hempel, J. C.; Morgan, L. O.; Lewis, W. B. *Inorg. Chem.* **1970**, *9*, 2064.

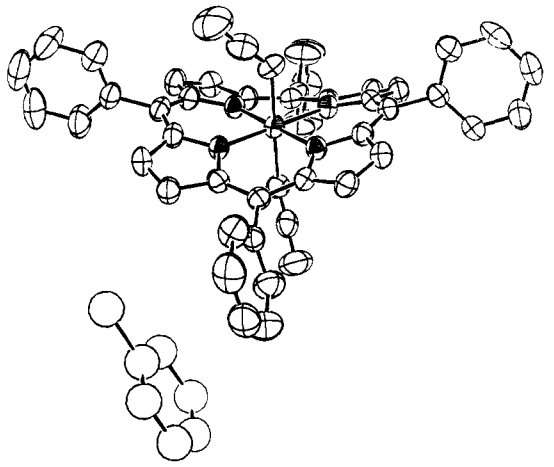

Figure 5. ORTEP[36] drawing of the $MnTPP(NCO)_2$ molecule showing the saddlelike ruffling of the porphyrin core (50% probability surfaces are shown).

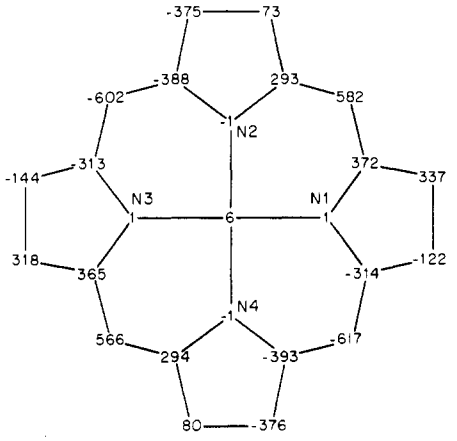

Figure 6. Diagram of the porphyrin core showing the perpendicular displacements from the mean N_4 plane in units of 0.001 Å. Positive displacements are toward NCO(B).

strongly distorted into a saddle shape, with quasi-S_4 ruffling[35] of the porphyrin core in crude accordance with D_{2d} point symmetry. An ORTEP[36] drawing of the $MnTPP(NCO)_2$ molecule showing the ruffling of the porphyrin core is given in Figure 5, and a diagram of the displacements of the core atoms from the mean N_4 plane is given in Figure 6. The pyrrole rings are planar (±0.02 Å) while the N_2C_3 bridging units are less planar (±0.05 Å). The primary distortion of the porphyrin core is the twist of the pyrrole rings about the Mn–N vectors. The tilt angles of the pyrrole groups with respect to the N_4 plane are all in the range of 18.6–18.9°. The pyrroles are also alternately tilted so as to point slightly toward opposite sides of the Mn atom. The displacements of the Mn atom from the mean pyrrole planes are 0.119, −0.146, 0.089, and −0.137 Å, for the pyrroles containing N1, N2, N3, and N4, respectively. The tilt angles of the N_2C_3 planes with respect to the N_4 plane are 15.8, 16.5, 15.5, and 16.7° for the planes containing C5, C10, C15, and C20, respectively. The maximum deviations of the porphyrin core atoms from the N_4 plane are ~±0.6 Å for the meso carbon atoms, C5, C10, C15, and C20.

The phenyl and toluene groups are planar.[21] The tilt angles of the phenyl groups from the N_4 plane are 73.6, 94.7, 96.1, and 74.1° for the phenyl groups attached at C5, C10, C15, and C20, respectively. The C–C distances in the toluene are meaningless due to the method used to model the disorder. The solvate fits into a hole in the packing of the porphyrin molecules (Figure S1).[21]

Discussion

The determination of the ground electronic state in oxidized metalloporphyrins is needed to understand their reactivity and properties. The one-electron oxidation of manganese(III) porphyrin complexes can occur either at the metal ion to give a manganese(IV) porphyrin complex or at the porphyrin ligand to give a manganese(III) porphyrin π cation radical. Kadish et al. recently reported that the one-electron electrochemical oxidation of a wide variety of $Mn^{III}TPP(X)$ species (X = ClO_4, I, NCS, Br, Cl, N_3) in the presence of Bu_4NClO_4 supporting electrolyte yielded only the manganese(III) porphyrin π cation radical species.[9b] The nearly invariant redox potential for the oxidations regardless of the axial ligand was consistent with ligand-centered oxidation. A representative complex, $[Mn^{III}TPP(Cl)]ClO_4$, was subsequently characterized by a variety of physical methods, which supported the formulation of a manganese(III) porphyrin π cation radical ground electronic state.[9a] We wish to demonstrate here that, with two more strongly coordinating axial ligands (e.g., N_3 or NCO), complexes with a Mn(IV) porphyrin ground electronic state are isolated and that the ground state in the Mn^{IV} porphyrin complexes is readily distinguished from the manganese(III) porphyrin π cation radical complexes by a variety of spectroscopic techniques.

Goff, Reed, and co-workers have reported that strong IR absorptions between 1270 and 1295 cm^{-1} are characteristic of a wide variety of tetraphenylporphyrin π cation radical complexes.[28] Strong bands at 1270 and 1290 cm^{-1} were reported for the Mn(III) porphyrin π cation radical complex $[Mn^{III}TPP(Cl)]ClO_4$.[28] The absence of any strong IR bands in this region in $MnTPP(NCO)_2$ and $MnTPP(N_3)_2$ indicates that ligand-centered oxidation has not occurred. On this basis, these complexes can tentatively be assigned a Mn(IV) ground electronic state. The room-temperature magnetic moments of **1** and **2** ($\mu_{eff} \approx 3.9\ \mu_B$) exclude a low-spin ($S = {}^1/_2$) Mn(IV) ground electronic state and are consistent with high-spin ($S = {}^3/_2$) Mn(IV). The magnetic moments of **1** and **2** are distinct from that reported for the Mn(III) porphyrin π cation radical complex $[Mn^{III}TPP(Cl)](ClO_4)$ ($\mu_{eff} = 4.7\ \mu_B$).[9a] The variable-temperature magnetic susceptibilities of **1** and **2** from room temperature to 5 K show no evidence for spin-state changes and are almost identical with that exhibited by the known high-spin d^3 complex $Mn^{IV}TPP(OCH_3)_2$[7] from which they were made (Figure 2).

The visible spectra of **1** and **2** (Figure 1) are similar to the visible spectrum of high-spin $Mn^{IV}TPP(OCH_3)_2$,[7] suggesting that they all have the same ground electronic state. The visible spectra of all three of these complexes ($\lambda_{max} = 419 \pm 3$ nm) are quite distinct from the spectra of the known Mn(III) porphyrin π cation radical complexes $[Mn^{III}TPP(Cl)](ClO_4)$[9a] and $[Mn^{III}TPP(Cl)](SbCl_6)$[37] ($\lambda_{max} \approx 390$ nm). The visible spectra of the monomeric complexes are qualitatively similar to those of the related dimeric complexes $[Mn^{IV}TPP(X)]_2O$ (X = N_3, NCO),[3b] indicating that they have similar electronic states. The existence of only small variations in the positions of the Soret bands in both the monomeric and the dimeric complexes indicates that interaction of the manganese ions through the oxo bridge does not significantly change the relative π-orbital energies within the porphyrin ring. However, the Soret bands in the dimers do have lower extinction coefficients (per manganese), and shoulders between 500 and 520

(35) Hoard, J. L. "Porphyrins and Metalloporphyrins"; Smith, K. M., Ed.; Elsevier: Amsterdam, 1975; p 317.
(36) Johnson, C. K. *Oak Ridge Natl. Lab., [Rep.] ORNL (U.S.)* **1965**, *ORNL-3794*.
(37) Scholz, W. R.; Reed, C. A., personal communication, University of Southern California, Nov 1982.

nm in the dimers are replaced by sharper peaks between 500 and 550 nm in the monomeric complexes.

Analysis of $Mn^{IV}TPP(NCO)_2$ Crystal Structure. An interesting feature of the structure of **2** is the severe quasi-S_4 ruffling[35] of the porphyrin core (Figures 5 and 6). The pyrrole rings are alternately twisted in opposite directions about the Mn–N bonds. The average tilt of the pyrrole rings from the N_4 plane is ±18.7°, and the average displacement of the meso carbon atoms (C5, C10, C15, C20) from the N_4 plane is ±0.59 Å. Only one other transition-metal tetraphenylporphyrin complex, $Co^{III}TPP(NO_2)$(3,5-lutidine), exhibits this much quasi-S_4 ruffling. In $Co^{III}TPP(NO_2)$(3,5-lutidine), the porphyrin ligand has not been oxidized and the ruffling of the porphyrin core was ascribed to crystal-packing forces.[38] The unusually large distortions of the porphyrin core in $Mn^{IV}TPP(NCO)_2$ can probably also be ascribed to crystal-packing forces. Of the 10 intermolecular contacts less than 3.5 Å, 3 involve the β-pyrrole carbon atoms and 7 involve the phenyl groups.[21] The ease of deformation of the porphyrin core in metalloporphyrins containing small metal ions (i.e. $M-N_{pyrrole} < 2.01$ Å) is demonstrated by the two crystalline modifications of $Ni^{II}OEP$.[5,39] The triclinic form of NiOEP has a nearly planar core with a $Ni-N_{av}$ distance of 1.958 Å whereas the tetragonal form exhibits a substantial S_4 ruffling such that the average displacement of the meso carbon atoms from the N_4 plane is 0.51 Å and the Ni–N distance is decreased to 1.929 Å. Neither crystalline form of NiOEP exhibits any unusually short (<3.5 Å) intermolecular contacts.[39] The large variation in the degree of ruffling within these two crystalline forms of the same molecule indicates one need not consider the porphyrin electronic state to explain even large degrees of this type of ruffling. Although the cause of the ruffling in **2** is not known, the ruffling can be adequately explained by the crystal-packing constraints. The severe ruffling of the porphyrin core in $Mn^{IV}TPP(NCO)_2$ contrasts with the nearly planar core in $Mn^{IV}TPP(OCH_3)_2$, where the molecules were more separated within the crystal lattice.[7] The difference in the average equatorial $Mn-N_{pyrrole}$ bond lengths of 0.045 Å can be attributed primarily to the differences in the degrees of porphyrin core ruffling in these two complexes.

The bond lengths about the Mn center in **2** are clearly distinct from those in six-coordinate high-spin Mn(III) porphyrin complexes, where very long axial bond lengths are observed due to the population of the antibonding d_{z^2} orbital.[27] The axial bond lengths in **2** are also shorter than the 2.186-Å $Mn-N_{imidazolate}$ bond lengths observed for what are believed to be low-spin Mn(III) ions at alternate sites in the polymeric complex $[Mn^{III}TPP(imidazolate)]_n$.[40] However, the presence of antiferromagnetic coupling, spin-state equilibria, and the polymeric nature of $[Mn^{III}TPP(Im)]_n$ may make these distances unrepresentative of low-spin Mn(III).[5] The complex $Bu_4N[Mn^{III}TPP(Im)_2]$ is the only low-spin Mn(III) porphyrin to be characterized to date, but the molecular structure of this compound has not been reported.[40] Until a structure of a monomeric low-spin Mn(III) porphyrin complex is determined, it will be difficult to distinguish with confidence between low-spin Mn(III) porphyrin π cation radical complexes and Mn(IV) porphyrin complexes on crystallographic grounds alone. However, it should be noted that the characteristic visible spectrum of high-spin $Mn^{III}TPP(NCO)$ did not change significantly when the complex was dissolved in dichloromethane containing 0.1 M $[Bu_4N]NCO$, indicating that association of two NCO ligands to form a low-spin Mn(III) complex is not favorable for this axial ligand.

The bond distances in **2** are consistent with manganese(IV). The axial $Mn-N_{NCO}$ distance of 1.926 Å in **2** is essentially identical with the $Fe-N_{azide}$ distance of 1.925 (7) Å found in low-spin $Fe^{III}TPP(N_3)(py)$,[26] consistent with the similar ionic radii of six-coordinate low-spin Fe(III) (r_{ionic} = 0.55 Å) and six-coordinate high-spin Mn(IV) (r_{ionic} = 0.53 Å)[41] and with the isoelectronic nature of the NCO and N_3 ligands. The difference between the $Fe-N_{pyrrole}$ distance of 1.989 Å and the $Mn-N_{pyrrole}$ distance of 1.970 Å is also in accordance with the differences in the ionic radii.

The internal bond distances of the isocyanate ligand in **2** are consistent with Mn–NCO vs. Mn–OCN binding. No terminal metallocyanate complexes have yet been characterized by X-ray crystallography,[42] but a substantial lengthening of the O–C bond of the OCN ligand compared to that of an N–C bond of an NCO ligand would be expected due to the sizable contribution of the $^-O-C\equiv N$ resonance structure. The short, average N–C distance of 1.167 Å found in **2** is comparable to that observed in $(Cp)_2Ti^{IV}(NCO)_2$ (N–C = 1.146 (23) Å), consistent with $^-N=C=O$ binding.[42] If the axial ligands were O bound, a short axial Mn–O distance similar to that seen in $Mn^{IV}TPP(OCH_3)_2$ (1.839 (2) Å)[7] would be expected, instead of the $Mn-N_{NCO}$ distance of 1.926 Å seen in **2**. The difference of 0.087 Å between the axial bond lengths in $Mn^{IV}TPP(NCO)_2$ and $Mn^{IV}TPP(OCH_3)_2$ can be directly ascribed to the differences in the axial ligands rather than to differences in the electronic states of the metals. A similar difference in axial bond distances (0.067 Å) is observed between the two high-spin complexes $Fe^{III}TPP(N_3)$[27] and $Fe^{III}MesoPDME(OCH_3)$.[5,43]

EPR Spectroscopy. Porphyrin π cation radical complexes are known to give strong EPR signals centered near $g = 2$.[44] The EPR spectrum of the π cation radical complex $[Mn^{III}TPP(Cl)](ClO_4)$ shows only a broad signal near $g = 2$, which has been suggested to be due to the relaxation of the porphyrin-centered radical induced by the Mn(III) ion.[9a] The EPR spectra of the complexes $MnTPP(X)_2$ (X = NCO, N_3, OCH_3) do not exhibit this broad signal at $g = 2$ but instead show highly anisotropic spectra (Figure 3) consistent with a high-spin d^3 ion in an environment of lower than O_h symmetry. The X-band EPR spectra of manganese(IV) porphyrin complexes appear to be qualitatively simpler than the complicated X-band EPR spectra of the isoelectronic chromium(III) tetraphenylporphyrin complexes $Cr^{III}TPP(Cl)(L)$ (L = one of a variety of neutral ligands).[45] The complexity of the Cr^{III} porphyrin EPR spectra is due to the presence of a tetragonal zero-field splitting parameter, D, that is smaller in magnitude than the microwave quantum ($h\nu \approx 0.31$ cm^{-1} for X-band). Since $|D|$ ranges from 0.145 to 0.245 cm^{-1} for the series of $Cr^{III}TPP(Cl)(L)$ species, transitions both within and between the two Kramers doublets are accessible. The presence of strong signals near $g = 4$ and the relative simplicity of the EPR spectra of the $Mn^{IV}TPP(X)_2$ complexes are indicative of the presence of a large zero-field splitting parameter, $|D| > h\nu$ (≈ 0.31 cm^{-1}), that prevents transitions between the upper and lower Kramers doublets from being accessible within the field range of the spectrometer. Spectra similar to those exhibited by the complexes $Mn^{IV}TPP(X)_2$ (with the hyperfine interaction

(38) Kaduk, J. A.; Scheidt, W. R. *Inorg. Chem.* **1974**, *13*, 1875.
(39) Cullen, D. L.; Meyer, E. F., Jr. *J. Am. Chem. Soc.* **1974**, *96*, 2095.
(40) Landrum, J. T.; Hatano, K.; Scheidt, W. R.; Reed, C. A. *J. Am. Chem. Soc.* **1980**, *102*, 6729.
(41) Shannon, R. D. *Acta Crystallogr., Sect. A: Cryst. Phys., Diffr., Theor. Gen. Crystallogr.* **1976**, *A32*, 751.
(42) Hargitta, I.; Paul, I. C. In "The Chemistry of Cyanates and Their Thio Derivatives"; Patai, S., Ed.; Wiley: New York, 1977; Part 1, Chapter 2.
(43) Hoard, J. L.; Hamor, M. J.; Hamor, T. A.; Caughey, W. S. *J. Am. Chem. Soc.* **1965**, *87*, 2312.
(44) (a) Subramanian, J. In "Porphyrins and Metalloporphyrins"; Smith, K., Ed.; Elsevier: Amsterdam, 1975; Chapter 13. (b) Fajer, J.; Davis, M. S. In "The Porphyrins"; Dolphin, D., Ed.; Academic Press: New York, 1979; Vol. IV, Chapter 4.
(45) Sommerville, D. A.; Jones, R. D.; Hoffman, B. M.; Basolo, F. *J. Am. Chem. Soc.* **1977**, *99*, 8195.

with the $I = {}^5/_2$ ^{55}Mn nucleus being ignored) have been reported for the series of tetragonally distorted pseudooctahedral d^3 complexes $[trans\text{-}Cr^{III}(L)_4XY]^+$ (L = pyridine or ammonia; X, Y = a wide variety of halogens and pseudohalogens)[46] and the series of rhombically anisotropic complexes $[trans\text{-}Cr^{III}(en)_2X_2]^{+,3+}$ (X = Cl, NCS, OH, H_2O).[5,34] Simulations of the EPR spectra and calculations of the resonant field positions' dependence on the zero-field splitting parameters for d^3 complexes have also been reported in the literature. An analysis of these EPR spectra and the published calculations indicates that transitions of at least moderate intensity can be expected between 5 and 10 kG in the X-band EPR spectra of d^3 complexes with $0.31\ cm^{-1} < |D| < 0.6\ cm^{-1}$.[34,46] When $|D| >> 0.6\ cm^{-1}$, these transitions can no longer be observed. The absence of transitions between 5 and 10 kG for the complexes $Mn^{IV}TPP(X)_2$ (X = OCH_3, N_3, NCO) indicates that $|D| > 0.6\ cm^{-1}$ for all of these complexes.

In the complex $Mn^{IV}TPP(NCO)_2$, the presence of transitions at $g \approx 2$ and $g \approx 4$ and the shape of the $g \approx 4$ transition are indicative of axial symmetry, i.e., $\lambda = E/D \approx 0$. If axial symmetry and an isotropic g value, $g_\perp = g_\parallel = 2.00$, are assumed, the value of D may be calculated by the equation[47]

$$D^2 \approx {}^3/_8[g_\perp(g_\perp\beta H)^2]/(2g_\perp - g_\perp{}^e)$$

If the value $g_\perp{}^e = 3.92$ from Figure 3c is used, the estimated value $|D| \approx 1.7\ cm^{-1}$ is calculated. It should be noted that the value of $|D|$ calculated by using this equation when $|D|$ is large (i.e. when $2g_\perp \approx g_\perp{}^e$) is very sensitive to the choice of the $g_\perp{}^e$ value from the experimental spectrum. Hence, this is only a crude estimate of $|D|$. The determination of the Q-band EPR spectra and the determination of low-temperature intensity measurements at $kT \approx |2D|$ are needed to determine more accurately the value and sign of D. An axial EPR spectrum with g values similar to those observed in $Mn^{IV}TPP(NCO)_2$ has recently been reported for a Mn^{IV} porphyrin complex, believed to be $Mn^{IV}TPP(Cl)_2$, that is formed by γ irradiation of $Mn^{III}TPP(Cl)$.[48]

In contrast with the axial EPR spectrum exhibited by $Mn^{IV}TPP(NCO)_2$, the EPR spectra of $Mn^{IV}TPP(OCH_3)_2$ and $Mn^{IV}TPP(N_3)_2$ are characteristically rhombic. The uncertainties in the effective g values in the spectra do not allow a quantitative analysis of the zero-field splitting parameters. However, the narrow range for $|D|$ found in the $Cr^{III}TPP(Cl)(L)$ complexes ($0.145\ cm^{-1} < |D| < 0.245\ cm^{-1}$),[45] despite coordination by C, N, O, and S donor ligands suggests that the Mn(IV) porphyrin complexes may also exhibit a small range of $|D|$ values. The existence of large zero-field splittings in all of the Mn(IV) porphyrins compared to those found in the Cr(III) porphyrins suggests that they are due to contraction along the axial bonds caused by the smaller ionic radius and higher charge of the Mn(IV) ion. A very rhombic EPR spectrum reported for $Mn^{IV}TPP(O_2)$ ($\lambda \approx {}^1/_3$)[6] is similar to that of $Mn^{IV}TPP(OCH_3)_2$. Similar EPR spectra have also been reported for the complex $(Me_4N)_2Mn^{IV}(sorbitolate)_3$.[49]

The EPR spectra of $Mn^{IV}TPP(OCH_3)_2$ and $Mn^{IV}TPP(NCO)_2$ show hyperfine coupling to the $I = {}^5/_2$ ^{55}Mn nucleus (a_{Mn} = 72 G for $Mn^{IV}TPP(OCH_3)_2$ and 69 G for $Mn^{IV}TPP(NCO)_2$) with magnitude comparable to that observed for Mn^{IV} in Al_2O_3 (a_{Mn} = 75 G).[50] The reduction of the coupling to the Mn nucleus may reflect a higher degree of covalency in these Mn^{IV} porphyrin complexes.

Conclusions. The properties of the complexes $MnTPP(X)_2$ (X = N_3, NCO, OCH_3) are consistent only with a high-spin Mn(IV) porphyrin ground electronic state. The EPR, IR, and electronic spectra are readily distinguishable from known Mn(III) porphyrin π cation radical complexes. The existence of at least two distinct electronic states for the products of one-electron oxidation of Mn(III) porphyrin complexes demonstrates that the electronic state can be controlled by the axial ligation. The Mn(IV) complexes are formed when the axial ligands are both good donors capable of stabilizing high oxidation states. When at least one ligand has very poor coordinating ability, e.g. ClO_4 or $SbCl_6$, ligand-centered oxidation may occur before the metal-centered oxidation. Electrochemical studies of the axial ligand dependence of the site of oxidation of Mn(III) porphyrin complexes are currently in progress in our laboratories.[51]

One system that utilizes manganese porphyrin complexes as catalysts to oxidize alkanes to alkyl azides has recently been reported.[2b] The visible spectrum reported for the manganese porphyrin intermediates during the catalysis is consistent with the presence of $Mn^{IV}TPP(N_3)_2$.[52] The EPR spectrum from another system that utilizes high-valent manganese porphyrin complexes for the oxidation of alkanes has also demonstrated the presence of monomeric manganese(IV) porphyrin intermediates,[2a] and a monomeric complex, $[PhIO(OAc)]_2Mn^{IV}TPP$, has recently been isolated from this system.[3a] The spectroscopic characterization of monomeric manganese(IV) porphyrin complexes described herein should aid the study of their role in the reactions where they are present.

Acknowledgment. Support of this work by the donors of the Petroleum Research Fund, administered by the American Chemical Society, and by Chevron Research Corp. is gratefully acknowledged. We are especially grateful to James Roe for invaluable aid in the interpretation of the EPR spectra and to John McCracken for assistance with the EPR spectrometer. The crystal structure analysis was performed at the UC Berkeley X-ray crystallographic facility (CHEXRAY).

Registry No. **1**, 87337-87-9; **2**, 87337-88-0; **2**·${}^1/_2C_6H_5CH_3$, 87337-89-1; $Mn^{IV}TPP(OCH_3)_2$, 83095-80-1.

Supplementary Material Available: Crystallographic data for $Mn^{IV}TPP(NCO)_2$·${}^1/_2C_6H_5CH_3$ including listings of observed and calculated structure factor amplitudes, nonessential bond distances and angles including those within the phenyl groups and the toluene solvate, anisotropic thermal parameters for non-hydrogen atoms, final hydrogen atom positional and thermal parameters, least-squares planes, and intermolecular contacts and a stereopair drawing of the unit cell, in addition to infrared spectra and a table of magnetic susceptibility data for $Mn^{IV}TPP(NCO)_2$ and $Mn^{IV}TPP(N_3)_2$ (44 pages). Ordering information is given on any current masthead page.

(46) Pedersen, E.; Toftlund, H. *Inorg. Chem.* **1974**, *13*, 1603.
(47) Ferrante, R. F.; Wilkerson, J. L.; Graham, W. R. M.; Weltner, W., Jr. *J. Chem. Phys.* **1977**, *67*, 5904.
(48) Konishi, S.; Hoshino, M.; Imamura, M. *J. Phys. Chem.* **1982**, *86*, 4537.
(49) Richens, D. T.; Sawyer, D. T. *J. Am. Chem. Soc.* **1979**, *101*, 3681.
(50) (a) Geschwind, S.; Kisliuk, P.; Klein, M. P.; Reinneika, J. P.; Wood, D. L. *Phys. Rev.* **1962**, *126*, 1684. (b) Cooper, S. R.; Dismukes, G. C.; Klein, M.; Calvin, M. *J. Am. Chem. Soc.* **1978**, *100*, 7248.
(51) Balfe, C. A.; Hill, C. L., unpublished results.
(52) Hill, C. L.; Smegal, J. A.; Henly, T. J. *J. Org. Chem.* **1983**, *48*, 3277.